Available online at www.sciencedirect.com
SCIENCE DIRECT
Polyhedron 25 (2006) 2039–2054
POLYHEDRON
www.elsevier.com/locate/poly

Molecular engineering of coordination pockets in chloro-tris-phenoxo complexes of titanium(IV)

Alastair J. Nielson *, Chaohong Shen, Joyce M. Waters

Chemistry, Institute of Fundamental Sciences, Massey University at Albany, Private Bag 102904, North Shore Mail Centre, Auckland, New Zealand

Received 6 December 2005; accepted 29 December 2005
Available online 28 February 2006

Abstract

The chloro-tris-phenoxo complexes [TiCl(OAr)$_3$] (OAr = $OC_6H_4CMe_3$-4 (**1**), $OC_6H_3Me_2$-2,4 (**2**), $OC_6H_2Me_3$-2,4,6 (**4**), $OC_6H_3(CHMe_2)_2$-2,6 (**5**), $OC_6H_3(CMe_3)_2$-2,4 (**6**) and OC_6H_4Ph-2 (**8**) are prepared by heating 3 equivalents of the phenol and [$TiCl_4$] in toluene. X-ray crystal structure determinations show that **2** is a phenoxy-bridged dimer with the *ortho*-methyl groups making the beginning of a pocket about the terminal chloro ligand and **6** is a tetrahedral monomer in which the pocket is more well developed by the *ortho-tert*-butyl groups. Both **2** and **6** react with dmbipy to give [TiCl(OAr)$_3$(dmbipy)] [OAr = $OC_6H_3Me_2$-2,4 (**3**) and $OC_6H_3(CMe_3)_2$-2,4 (**7**)] in which the original pocket is destroyed. Reaction of $TiCl_4$ with 3 equivalents of $LiOC_6H_4Ph$-2 in diethyl ether gives [TiCl(OC_6H_4Ph-2)$_3$(diethyl ether)] (**9**) for which an X-ray crystal structure determination shows a trigonal bipyramidal coordination geometry with the diethyl ether lying *trans* to the chloro ligand. The three phenoxide ligands make up the equatorial plane which takes the 2-phenyl substituent on each phenoxo ligand away from the chloro ligand resulting in a partially collapsed cavity. The tied-back analogues of **2** and **6**, [TiCl{($OC_6H_2Me_2$-2,4-CH_2-6)$_3$N}] (**11**) and [TiCl({$OC_6H_2(CMe_3)_2$-2,4-CH_2-6}$_3$N)]·diethyl ether (**12**), are prepared by adding $(HOArCH_2)_3N$ [Ar = $C_6H_2Me_2$-2,4 and $C_6H_2(CMe_3)_2$ 2,4] to [TiCl($OCHMe_2$)$_3$] in diethyl ether. An X-ray crystal structure of **12** showed a trigonal bipyramidal structure with a coordination environment about the terminal chloro ligand similar to that found in **6**. Complex **12** reacts with pyridine to form the 6-coordinate complex [TiCl({$OC_6H_2(CMe_3)_2$-2,4-CH_2-6}$_3$N)(py)] (**13**).

Keywords: Ti(IV); Phenoxo ligands; Coordination pockets; Crystal structures

1. Introduction

The formation of transition metal complexes where ligand systems are designed to form cavities or pockets in which another ligand sits, is an area of growing interest [1]. The impetus for the preparation of these metallopockets has come from the desire to form small molecule complexes that resemble the metal-containing pockets present in metalloproteins and enzymes [2,3]. Presently, there is interest in molecular engineering of metallopockets that might be important for organic reaction catalysis in non-aqueous media [4]. A related area is the formation of metalloclefts [5] for catalysis [6] and molecular recognition [7]. Where non-collapsible pockets are required in the biological field, tied-back tripodal ligands have been used to good effect either where the tie-back atom is not involved in bonding to the metal such as in the case of bulky tris-(pyrazoyl)borate ligands [8] or where it coordinates to the metal as in the case of tris(carbamoyl)methyl amine [9]. In the non-biological area, tied-back triamido ligands, $[(RNCH_2CH_2)_3N]^{3-}$, have been used to make steric pressure pockets useful in the catalytic reduction of dinitrogen [10] and non-tied back triamido complexes are also showing interesting chemistry [11].

There is growing evidence that chloro-tris-phenoxo complexes of titanium(IV), [TiCl(OAr)$_3$], have a coordination environment that allows selectivity in organic reactions. [TiCl(OC_6H_5)$_3$], which has been known for some time [12] has been used in regioselective and stereoselective ring allylation of epoxides [13,14] and diastereoselective allylation of ketones [15]. Recently, [TiCl($OC_6H_3Ph_2$-2,6)$_3$]

* Corresponding author.
E-mail address: a.j.nielson@massey.ac.nz (A.J. Nielson).

0277-5387/$ - see front matter © 2006 Elsevier Ltd. All rights reserved.
doi:10.1016/j.poly.2005.12.027

was prepared and used as a catalyst precursor for epoxide ring opening [16]. This reaction makes use of bulky 2,6 substituents to create a pocket in a similar manner to the designer Lewis acid catalysts based on aluminium tris-phenoxo complexes [17]. For these reactions the influence of local coordination environment is important and this can be varied more easily by changing substituents on the aromatic ring of phenoxo ligands than it can with the alkoxo ligands in the complexes $[TiCl(OR)_3]$ which also have an extensive use in organic synthesis [18]. However, chloro-tris-phenoxo complexes containing *ortho*-phenyl ring substituents are not well known. $[TiCl(OC_6H_2Me_3\text{-}2,4,6)_3]$ has been prepared [19,20] and some bis-amine adducts formed [20]. $[TiCl\{OC_6H_3(CHMe_2)_2\text{-}2,6\}_3]$ has been briefly described [20,21] and the X-ray structure of $[TiCl\{OC_6H_3(CMe_3)_2\text{-}2,6\}_3]$ obtained [22]. We report here work that is based on identifying pockets in chloro-tris-phenoxo complexes of titanium(IV) and investigate how this site topology may be retained.

2. Results and discussion

We have found that the best method for preparing the chloro-tris-phenoxo complexes even when there is a relatively large *ortho*-substituent on the phenyl ring is to simply thermalise the phenol and $[TiCl_4]$ in toluene (Eq. (1)).

$$[TiCl_4] + 3ArOH \rightarrow [TiCl(OAr)_3] + 3HCl \quad (1)$$

$$\begin{aligned} OAr = {} & OC_6H_4CMe_3\text{-}4, \\ & OC_6H_3Me_2\text{-}2,4, \\ & OC_6H_2Me_3\text{-}2,4,6, \\ & OC_6H_3(CHMe_2)_2\text{-}2,6, \\ & OC_6H_3(CMe_3)_2\text{-}2,4, \\ & OC_6H_4Ph\text{-}2. \end{aligned}$$

Obtaining very high yields relies on reaching the reaction end-point and this can be easily determined by monitoring the HCl exhaust gas production using amine hydrochloride cloud formation. This has been found to be successful for the general preparation of mono and bis-phenoxo complexes of titanium [23,24].

To ascertain the features associated with a chloro-tris-phenoxo complex in which there are no *ortho*-substituents on the phenyl ring, the reaction of 4-*tert*-butylphenol and $[TiCl_4]$ in a 3:1 ratio was undertaken. The production of HCl gas was vigorous at first but the reaction took 35 h for the last traces of HCl to be expelled. After removing the solvent, a non-crystalline material was obtained which failed to crystallise. Analytical data and the NMR spectra showed that even after extended periods of drying in vacuo, the complex retained toluene solvate and was characterised as $[TiCl(OC_6H_4CMe_3\text{-}4)_3] \cdot 0.5C_7H_8$ (**1**). Both the ^1H NMR and $^{13}C\{^1H\}$ NMR spectra showed the toluene as well-defined resonances whereas the 4-*tert*-butylphenoxo ligand resonances were broad suggesting solution dynamics [24]. In particular, the *ipso*-carbon resonance occurred at δ 164.5 which is upfield of that found for the mono-phenoxo complex $[TiCl_3(OC_6H_4CMe_3\text{-}4)]$ (δ 169.7) [23] and the bis-phenoxide complex $[TiCl_2(OC_6H_4CMe_3\text{-}4)_2]$ (δ 166.3) and is likely to represent a decrease in the π-bonding from each phenoxo ligand when the number of these ligands increases [24].

When $[TiCl_4]$ was reacted with 2,4-dimethylphenol using the standard conditions, a crystalline solid analysing as $[TiCl(OC_6H_3Me_2\text{-}2,4)_3]$ was obtained for which an X-ray crystal structure determination showed the dimeric phenoxo bridged complex **2**. The coordination geometry about each Ti is that of a trigonal bipyramid consisting of two bridging phenoxides, two terminal phenoxides and a terminal chloro ligand (Fig. 1a). Bond lengths and angles are shown in Table 1. The Ti–O(3) bond length [1.757(1) Å] is similar to that found in the mono-phenoxo complex $[TiCl_3\{OC_6H_2(CMe_3)_2\text{-}2,6\text{-}Me\text{-}4\}]$ [Ti–O bond length 1.750(2) Å] for which a theoretical study shows π-donation of both oxygen atom lone pairs to titanium and some π-bonding between the oxygen and the phenyl ring π-system [24]. The Ti–O(3)–C(31) bond angle [171.4(1)°] in **2** is more 'linear' than that found in $[TiCl_3\{OC_6H_2(CMe_3)_2\text{-}2,6\text{-}Me\text{-}4\}]$ [163.1(1)°] for which theoretical studies show significant changes in energy (and thus decrease in O_π–Ti_d donation) occur only after the Ti–O–C bond angle moves below ca. 160°. The Ti–O(2) bond length in **2** [1.794(2) Å] is significantly longer than the Ti–O(3) bond length and the Ti–O(2)–C(21) bond angle decreases to 138.8(1)° reflecting the decreased π-donation from the oxygen of this ligand. The Ti–O(1) bond length of 1.927(1) Å and Ti–O(1)–C(11) bond angle of 126.1(1)° suggest that there is minimal π-donation to Ti with the bridging phenoxo ligand. The bond length of the terminal chloro ligand [2.269(1) Å] is appreciably longer than that observed for the two terminal chloro ligands in the bridging phenoxo complex $[\{TiCl_2(OC_6H_4CMe_3\text{-}4)(\mu\text{-}OC_6H_4CMe_3\text{-}4)_2\}_2]$ [2.2186(11) and 2.2256(11) Å] [24] as a result of the lessened need for Cl_p–Ti_d π-donation when there is a third phenoxo ligand present.

For chloro-tris-phenoxo complexes, the local environment of the terminal chloro ligand is of importance when development of a pocket is considered since it is this ligand and any replacement that will be affected by local steric influences. Inspection of **2** and the space-filled model (Fig. 1b) shows that the orientation of the phenyl rings in the solid state is such that the methyl substituents in the *ortho*-positions of the three phenoxo ligands associated with each of the titanium atoms point up towards the terminal chloro ligand and as such start to build a 'wall' around one side of the upper Ti(1)–Cl bond but do not create a significant pocket. In fact the phenyl rings attached to the adjacent Ti atom create more of a wall but are further away from the chloro ligand. In solution, the influences playing on the chloro ligand would appear to be different from the solid state since the NMR spectra of **2** in $CDCl_3$ solution do not reflect the dimeric structure shown by the X-ray analysis but point to the three phenoxides being

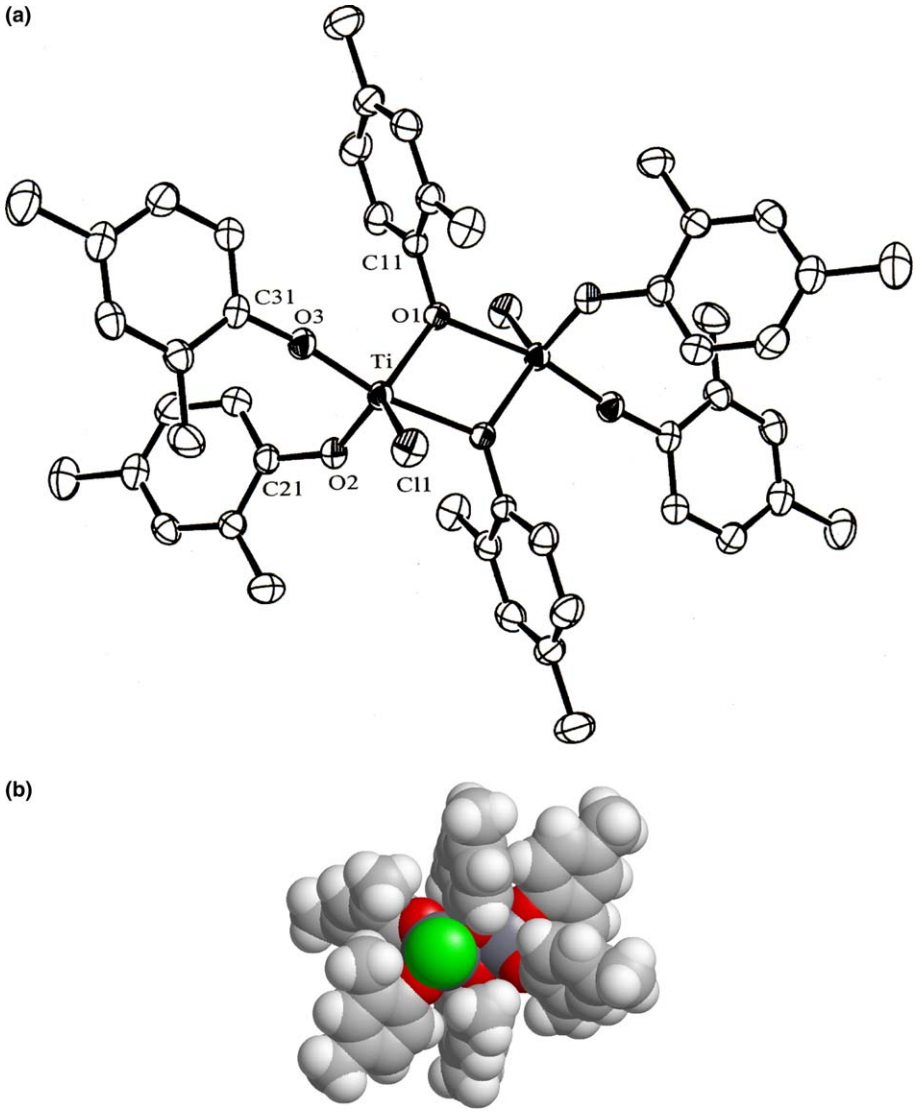

Fig. 1. (a) ORTEP diagram of [{TiCl($OC_6H_3Me_2$-2,4)$_2$(μ-$OC_6H_3Me_2$-2,4)}$_2$] (**2**) showing the molecular structure. Hydrogen atoms have been omitted for clarity. Only the major coordination site for Cl is shown. (b) Space-filling model looking down the Cl–Ti bond showing the position of the *o*-methyl groups on the Ti(1) phenoxo ligands and the phenoxo phenyl groups on Ti(2).

equivalent. The ^{1}H NMR spectrum shows a single set of sharp resonances for the *ortho* and *para*-methyls, a multiplet for the two *meta*-phenyl ring hydrogens and the $^{13}C\{^1H\}$ NMR spectrum a single set of resonances for the relevant phenoxide group carbons. The *ipso*-carbon resonance appears at δ 164.4 which is in a position similar to that found for **1** (δ 164.5). The absence of resonances for bridging and terminal ligands and the sharpened nature of the resonances suggest that solution dynamics are less important than for **1** so that the complex is likely to be monomeric in the NMR solvent and have a tetrahedral geometry in which the *ortho*-methyl groups all point up around the Ti–Cl bond. In comparison, the resonances of complex **1**, particularly those associated with the aromatic ring, were broad which may suggest monomer–dimer equilibria. We have found previously that [$TiCl_2(OAr)_2$] complexes without *ortho*-methyl substituents are dimeric in the solid state but are monomeric in solution. DFT calculations show that there is only a small dimerisation energy involved (-26.2 kJ mol^{-1}) [24].

Of fundamental importance in these systems is whether the structure of any pocket is maintained in the presence of other coordinating ligands. Addition of one or two equivalents of pyridine to **2** gave what appeared to be isomeric mixtures, which were difficult to distinguish by NMR spectroscopy. 4,4′-Dimethyl-2,2′-bipyridine (dmbipy) was used since isomeric mixtures can be more easily identified using this ligand [23,24]. Addition to **2** expanded the coordination number giving [TiCl($OC_6H_3Me_2$-2,4)$_3$(dmbipy)] (**3**) for which the NMR spectra showed one isomer. Based on a 2:1 ratio of phenoxo ligand resonances and a symmetrical dmbipy ligand shown by a singlet for the two methyl groups and a single set of resonances for the ring protons in the ^{1}H NMR spectrum and the required number of carbon resonances in the $^{13}C\{^1H\}$ NMR spectrum, dmbipy symmetric structure (a) rather than either of asymmetric

Table 1
Selected bond distances (Å) and angles (°) for [{TiCl($OC_6H_3Me_2$-2,4)$_2$-(μ-$OC_6H_3Me_2$-2,4)}$_2$] (**2**)

Ti–Cl(1)	2.269(1)
Ti–O(1)	1.927(1)
Ti–O(2)	1.794(2)
Ti–O(3)	1.757(1)
Ti–O(1)′	2.138(1)
Ti–O(1)–C(11)	126.1(1)
Ti–O(2)–C(21)	138.8(1)
Ti–O(3)–C(31)	171.4(1)
Ti–O(1)′–C(11)′	125.6(1)
Cl(1)–Ti–O(1)	121.21(7)
Cl(1)–Ti–O(2)	115.90(8)
Cl(1)–Ti–O(3)	96.86(5)
Cl(1)–Ti–O(1)′	89.75(4)
O(1)–Ti–O(1)′	71.76(6)
O(1)–Ti–O(2)	118.23(7)
O(1)–Ti–O(3)	95.89(6)
O(2)–Ti–O(1)′	87.41(6)
O(2)–Ti–O(3)	98.96(7)
O(3)–Ti–O(1)′	167.65(6)
Ti–O(1)–Ti′	108.24(6)

structures (b) and (c) is preferred. We have been unable to obtain suitable crystals to identify the absolute structure in the isomer but with one phenoxo ligand coordinating *trans*- to the chloro ligand the cavity structure about Cl is certainly destroyed.

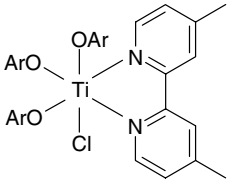

Symmetric structure (a)

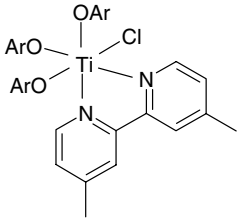

Asymmetric structure (b)

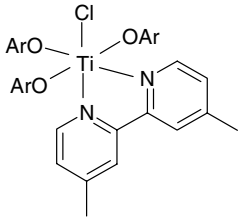

Asymmetric structure (c)

The structural features shown by the solid state structure of **2** indicate that one side of the titanium has become enclosed to some extent by the phenoxo ligand *ortho*-methyl groups so that the complex has the beginnings of a pocket with defined local structure. A more well-defined topology could arise if the complex were a tetrahedral monomer as suggested by the NMR spectra. However, analysis of the structure indicates that some rotation of the phenyl C–O bonds in the monomer or dimer forms may occur in solution taking the methyl groups away from the chloro ligand. Thus, 2,4,6-trimethylphenol and 2,6-di-*iso*-propylphenol were reacted with $TiCl_4$ using the standard conditions to form complexes in which phenoxo ligand C–O bond rotations are less likely to occur on account of the other *ortho*-position of the phenyl ring having a larger substituent than hydrogen. [TiCl($OC_6H_2Me_3$-2,4,6)$_3$] (**4**) [19] formed as a solid which, characterised by NMR spectroscopy, showed a single set of sharp resonances for the relevant hydrogens and carbons as found for complex **2** and with an *ipso*-carbon resonance in the $^{13}C\{^1H\}$ NMR spectrum at δ 163.9 suggesting a monomeric and thus tetrahedral complex. [TiCl{OC_6H_3-($CHMe_2$)$_2$-2,6}$_3$] (**5**) [20,21] was characterised by NMR spectral comparison with the product formed by thermalisation in benzene [21] as NMR analysis of the toluene reaction crude material indicated there was a significant amount of the phenol present as well as the *tetra*-phenoxide [Ti{$OC_6H_3(CHMe_2)_2$-2,6}$_4$] (identified by NMR spectral comparison with an independently prepared sample). Based on the single set of ligand resonances in the NMR spectra (in particular the *ipso*-carbon ^{13}C resonance at δ 163.1) **5** is also a tetrahedral monomer.

Of more importance than methyl or *iso*-propyl groups for pocket development are large *ortho*-substituents. The X-ray structures of [TiI{$OC_6H_3(CMe_3)_2$-2,6}$_3$] [22] and [TiCl($OC_6H_3Ph_2$-2,6)$_3$] [16] show cavity formation and would appear to be ideal molecules for cavity collapse studies. However, the former complex is difficult to prepare and the ligand for the latter is expensive. We therefore turned our attention to ligands that had a *tert*-butyl or phenyl substituent in only one of the phenoxide aryl ring *ortho*-positions. Reaction of 2,4-di-*tert*-butylphenol with [$TiCl_4$] under the standard conditions gave [TiCl{OC_6H_3-(CMe_3)$_2$-2,4}$_3$] (**6**) which could also be prepared in good yield by the reaction of 3 equivalents of $LiOC_6H_3$-(CMe_3)$_2$-2,4 with $TiCl_4$ dissolved in diethyl ether. The complex forms a crystalline mass that is analytically pure when the solvent is removed from the reaction mixture but may be recrystallised from petroleum spirit or diethyl ether. An X-ray crystal structure determination showed a distorted tetrahedron consisting of three terminal phenoxo ligands and a single terminal chloro ligand (Fig. 2a), the metal and chloro ligand lying along a threefold axis. Bond lengths and angle are shown in Table 2. The three identical Ti–O bond lengths [1.757(2) Å] are similar to the Ti–O(3) bond length in **2** which involves the most oxygen atom lone pair π-donation. The Ti–Cl bond length in **6** [2.240(2) Å] is slightly shorter than that observed in **2** [2.269(1) Å] resulting from the greater need for electron density at the metal with the lower coordination number. It is considerably shorter than the three terminal Ti–Cl bonds in [$TiCl_3${$OC_6H_2(CMe_3)_2$-2,6-Me-4}] [Ti–Cl bond length range 2.1822(8)–2.1945(9) Å] in which there is only one π-donating phenoxo ligand. In [$TiCl_4$] where each chloride must π-donate 2 electron pairs to attain an electron count of 16, the Ti–Cl bond lengths are 2.170(2) Å [25].

The Ti–O–C bond angles in **6** [158.8(2)°] are slightly smaller than those found in [$TiCl_3${$OC_6H_2(CMe_3)_2$-2,6-

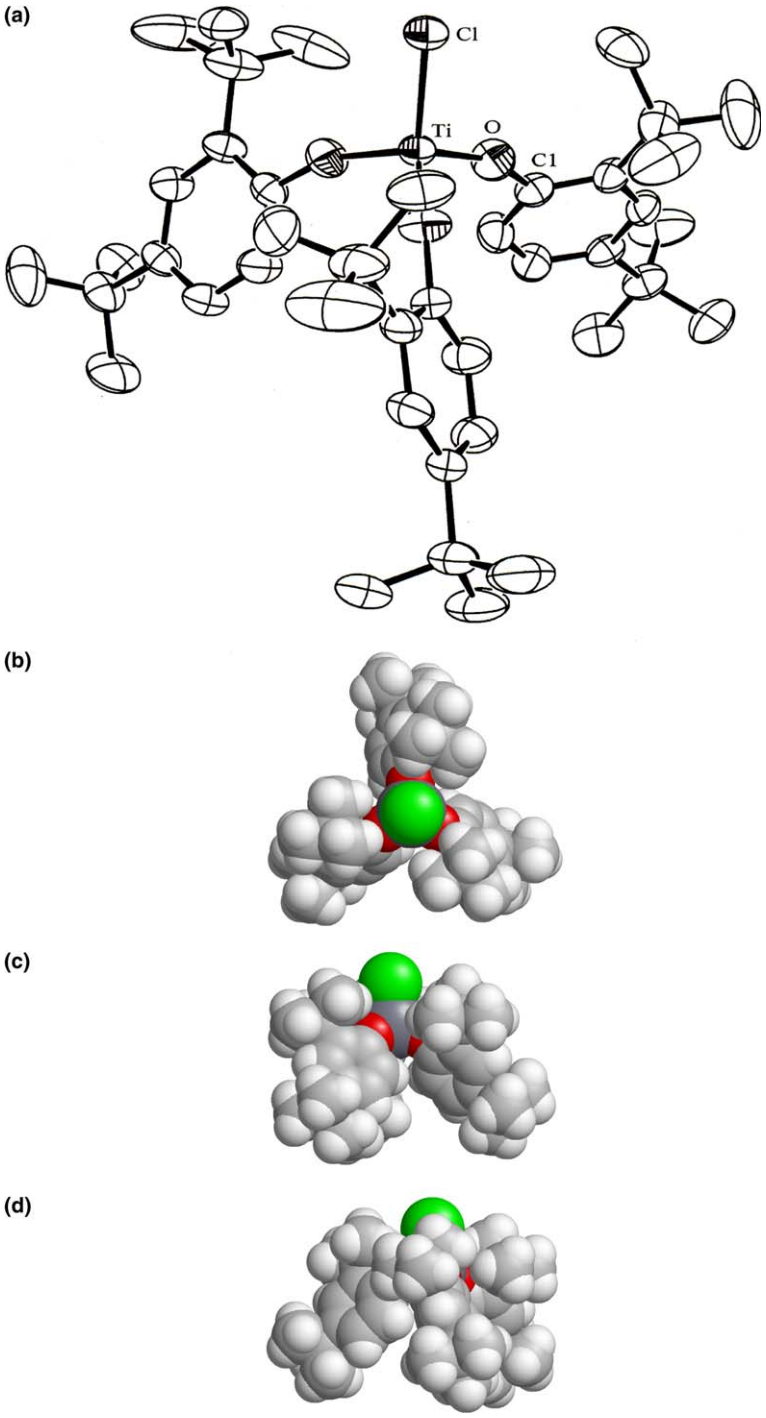

Fig. 2. (a) ORTEP diagram of $[TiCl\{OC_6H_3(CMe_3)_2\text{-}2,4\}_3]$ (**6**) showing the molecular structure. Hydrogen atoms are omitted for clarity. Only one of the disordered positions for the *tert*-butyl group is shown. (b) Space-filling model looking down the Cl–Ti bond showing the pocket arrangement about Cl. (c and d) Space-filling model, side-on view of the Ti–Cl bond showing the extent to which the *tert*-butyl group methyls cover the Cl atom.

Me-4}] [163.1(2)°] [23] and the Ti–O(3)–C(31) bond angle in complex **2** [171.4(1)°] but the angle in **6** is only a little less than the 160° for which theoretical studies with this type of ligand show a steep rise in energy when this value is reduced [23]. In $[TiI\{OC_6H_3(CMe_3)_2\text{-}2,6\}_3]$ where both phenyl ring *ortho*-positions have *tert*-butyl substituents the Ti–O–C bond angles range from 155.2(4)° to 158.2(4)° [22]. In **6** the O–Ti–O′ and O–Ti–Cl bond angles are 108.90(8)° and 110.03(8)°, respectively, hence the geometry does not deviate significantly from a tetrahedral arrangement. In $[TiI(OC_6H_3(CMe_3)_2\text{-}2,6)_3]$ the O–Ti–O bond angles range from 110.7(3)° to 114.9(3)° and the O–Ti–I bond angle range is 102.9(3)–108.6(3)° [22].

The phenyl rings in complex **6** orientate so that two of the methyl groups of the 2-*tert*-butyl group straddle the chloro ligand but lie slightly to the side of this ligand. The two closest methyl group carbon contacts with the chloro ligand are 3.13 and 3.11 Å which, taken with the

Table 2
Selected bond distances (Å) and angles (°) for [TiCl{$OC_6H_3(CMe_3)_2$-2,4}$_3$] (**6**)

Ti–Cl	2.240(2)
Ti–O(1)	1.757(2)
Ti–O(1)–C(1)	158.8(2)
Cl–Ti–O(1)	110.03(8)
O(1)–Ti–O(1)′	108.90(8)

Ti–O–C(1) bond angles [158.8(2)°], and the near ideal tetrahedral geometry, indicate that the 2-*tert*-butyl substituent exerts little steric pressure. However, it is more constrained than its counterpart in the 4-position of the phenyl ring which is seen to occupy two disordered sites. No such disorder was observed for the 2-substituent. It provides something of a steric shield about the chloro ligand and thus creates a pocket for this fourth coordination site as the space filled models show (Fig. 2b–d). Molecular models indicate that if the Ti–O–C bond angles are maintained in solution near the solid state value of ca. 159° then rotation about the phenyl ring C–O bond is difficult. However, since this angle can flatten with little energy consequence [23] rotation may be possible although the C–O π-bond would need to be broken in this process.

The 4-coordination of complex **6** can be broken by the addition of dmbipy but whereas the *ortho*-methyl complex **2** gave one product which NMR spectroscopy showed to have a symmetric structure, reaction with **6** gave a product analysing as [TiCl{$OC_6H_3(CMe_3)_2$-2,4}$_3$(dmbipy)] (**7**) but the NMR spectra showed three products (ratio ca. 72:21:7) based on the easily distinguished features of the dmbipy hydrogens in the ^{1}H NMR spectrum. The major product, however, had spectral characteristics similar to complex **3** [symmetric structure (a)]. Of the three possible structures only (c) has the potential for three *tert*-butyl groups to surround Cl. We have also looked at the possibility of coordinating only one extra ligand to **6** by adding 1 equivalent of pyridine or various aldehydes but these reactions give gummy substances that are hard to purify. However, the NMR spectra show mainly single resonances for the phenoxo ligands indicating the ligands are equivalent which offers the possibility of a 5-coordinate structure (see later).

The structural features shown by complex **6** suggest that the chloro ligand would sit in a more effective pocket if the 2-*tert*-butyl substituent of the phenoxo ligands were replaced by a 2-phenyl substituent which, although less sterically demanding than the former, would protrude further out. Reaction of 2-phenylphenol with [$TiCl_4$] under the standard conditions gave an oil which failed to solidify but was identified as [TiCl(OC_6H_4Ph-2)$_3$] (**8**) on the basis of its NMR spectra. In particular, the more easily identified ^{13}C{^{1}H} NMR spectrum showed a single set of resonances for each of the carbons of the ligand and the *ipso*-carbon resonance (δ 163.6) was in a similar position to the other chloro-tris-phenoxide complexes prepared.

Reaction of [$TiCl_4$] with 3 equivalents of $LiOC_6H_4$Ph-2 in diethyl ether gave [TiCl(OC_6H_4Ph-2)$_3$(diethyl ether)] (**9**) which had nearly identical NMR spectral characteristics in the aromatic region to those shown by complex **8** with the *ipso*-carbon at δ 163.2. Interestingly, when complex **8** was dissolved and refluxed in diethyl ether the NMR spectra of the reaction product indicated that no diethyl ether was incorporated. This is probably related to the retention of coordinated ether during the reaction with the titanium starting material [$TiCl_4$(diethylether)$_2$]. An X-ray crystal structure determination of **9** showed a distorted trigonal bipyramidal coordination geometry with the diethyl ether ligand bound in a *trans* position to the chloro ligand and the three phenoxide ligands forming the equatorial plane (Fig. 3a). Bond lengths and angle are shown in Table 3. The Ti–O bond lengths lie in the range 1.790(1)–1.794(1) Å and, together with the Ti–Cl bond length [2.3067(6) Å], are much longer than the corresponding bonds in [TiCl{$OC_6H_3(CMe_3)_2$-2,4}$_3$] (**6**) [Ti–O and Ti–Cl are 1.757(2) and 2.240(2) Å, respectively]. This is a result of **9** having a reduced π-loading [26] requirement compared to **8** with the addition of the 2-electon donor diethyl ether ligand. Consequently, the Ti–O–C bond angles of 152.3(1)°, 155.0(1)° and 157.1(1)° relax a little in comparison with those in **6** where Ti–O–C bond angle is 158.8(2)°. The phenoxide oxygen atoms push away from the chloro ligand [O(1)–Ti–Cl, 96.12(4)°; O(2)–Ti–Cl, 95.90(5)°] but the O–Ti–O bond angles are close to the ideal trigonal angle [the range is 117.88(6)–119.99(6)°]. The phenyl rings are rotated into the equatorial plane to remove interaction with the diethyl ether ligand and this takes the 2-phenyl substituent on each phenoxo ligand away from the chloro ligand and destroys any substantial cavity present if the substituents all lie upright. The space-filling model looking down the Cl–Ti bond (Fig. 3b) shows the cavity effect which is different from that observed in [TiCl($OC_6H_3Ph_2$-2,6)$_3$] [16] where the substituents form an open-ended groove (Fig. 3c). This results from a face-to-face orientation of two of the phenyl substituents and an end wall in which the substituent has moved aside slightly. The extent to which the phenyl groups cover the chloro ligand in **9** is much less than in [TiCl($OC_6H_3Ph_2$-2,6)$_3$] (compare Fig. 3d and e) being somewhat similar to that found in [TiCl{$OC_6H_3(CMe_3)_2$-2,4}$_3$] (**6**) (compare Fig. 3d with Fig. 2c).

The structural features shown by complexes **6** and **9** indicate that the local cavity geometry is easily effected by the addition of another ligand. We therefore looked at tying back one of the three phenoxo ligands with a nitrogen donor using the benzylamine ligand structure (d) to form complexes of structural type (e).

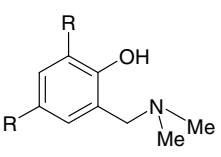

Structure (d) (R = CMe_3)

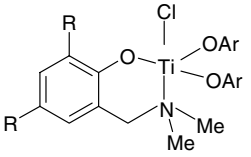

Structural type (e) (R = CMe_3)

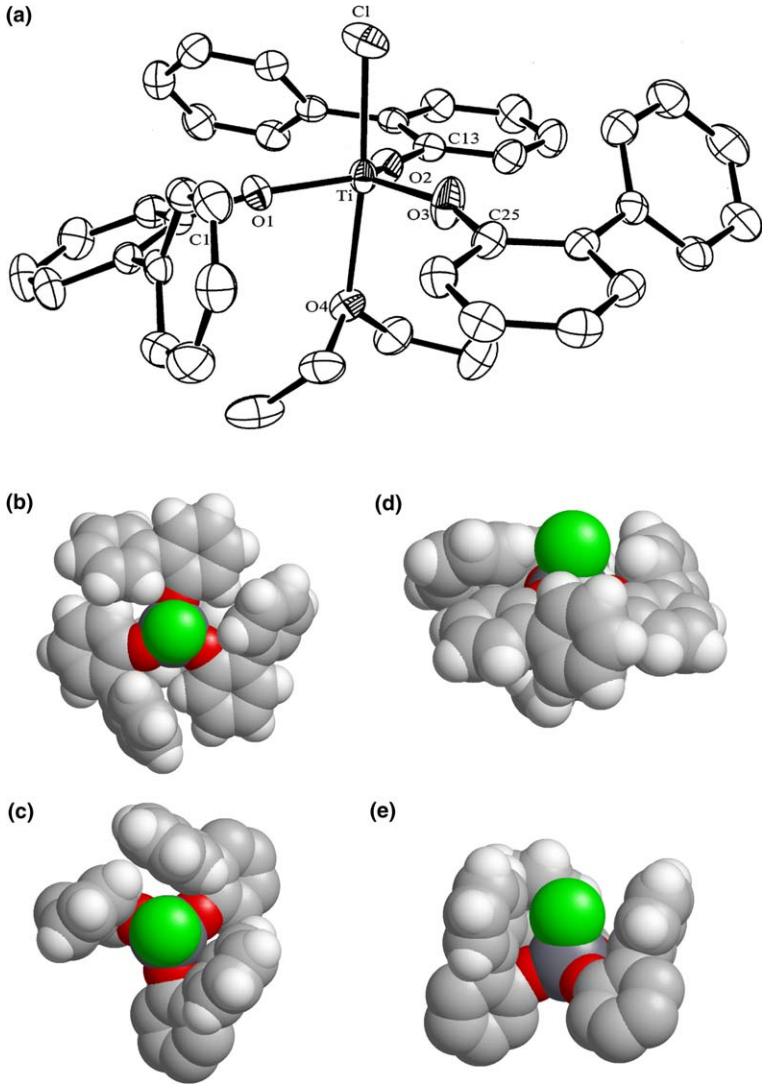

Fig. 3. (a) ORTEP diagram of [TiCl(OC_6H_4Ph-2)$_3$(diethyl ether)] (**9**) showing the molecular structure. Hydrogen atoms are omitted for clarity. Only the major site of the coordinated ether ligand is shown. (b) Space-filling model of **9** looking down the Cl–Ti bond showing the collapsed *o*-phenyl group arrangement about Cl. (c) Space-filling model of [TiCl($OC_6H_4Ph_2$-2,6)$_3$] [16] showing the upright *o*-phenyl groups and the resulting groove (the 6-phenyl groups and the phenoxo ligand Hs have been removed for clarity). (d) Space-filling model, side-on view of **9** showing the extent to which the *o*-phenyl groups cover Cl. (e) Space-filling model, side-on view of [TiCl($OC_6H_4Ph_2$-2,6)$_3$] [16] showing the molecular groove (the 6-phenyl groups and the phenoxo ligand Hs have been removed for clarity).

This approach is then expected to produce one rigid phenoxo ligand and two more that are less rigid if the isomer with Cl *trans* to N is formed, allowing the influences made on the cavity ligand to be varied. Preliminary results of this work indicate that reaction of [$TiCl_2$($OC_6H_4CMe_3$-4)$_2$] [24] with $LiOC_6H_2(CMe_3)_2$-2,4-(CH_2NMe_2)-6 gives a solid analysing as the complex [TiCl($OC_6H_4CMe_3$-4)$_2$-{$OC_6H_2(CMe_3)_2$-2,4-(CH_2NMe_2)-6}] but the NMR spectra show the complex is made up of two isomers. Similarly, reaction of [$TiCl_4$] with two equivalents of $LiOC_6H_3$-(CMe_3)$_2$-2,4 in diethyl ether followed by one equivalent of $LiOC_6H_2(CMe_3)_2$-2,4-(CH_2NMe_2)-6 gives a complex analysing as [TiCl{$OC_6H_4(CMe_3)_2$-2, 4}$_2$($OC_6H_2(CMe_3)_2$-2,4-(CH_2NMe_2)-6)] which was also shown by the NMR spectra to consist of two isomers. The complexes do not appear to crystallise from solution so the structural details of any cavity formed in any of the isomers cannot as yet be assessed. The only success we have had with forming a single isomer complex using this type of tie-back is from a reaction of [$TiCl_2$({$OC_6H_2(CMe_3)$-2-Me-4}$_2CH_2$-6)] [27] with one equivalent of $LiOC_6H_2(CMe_3)_2$-2,4-(CH_2NMe_2)-6 which gives a product analysing as [TiCl({$OC_6H_2(CMe_3)$-2-Me-4}$_2CH_2$-6) ($OC_6H_2(CMe_3)_2$-2,4-(CH_2NMe_2)-6)]. The NMR spectra indicate the presence of only one isomer but crystals have not yet been obtained to identify the overall geometry by X-ray crystallography.

In further pursuing a non-collapsible coordination geometry about titanium, we have looked at the coordination properties of the tripodal ligand type tris(2-hydroxyphenyl)benzylamine, ($HOArCH_2$)$_3$N) for which the methyl and *tert*-butyl substituted compounds (HOC_6H_2-Me_2-2,4-CH_2-6)$_3$N [structure (f), R = Me] and

Table 3
Selected bond distances (Å) and angles (°) for [TiCl(OC$_6$H$_4$Ph-2)$_3$(diethyl ether)] (**9**)

Ti–Cl	2.3067(6)
Ti–O(1)	1.791(1)
Ti–O(2)	1.794(1)
Ti–O(3)	1.790(1)
Ti–O(4)	2.312(3)
Ti–O(1)–C(1)	152.3(1)
Ti–O(2)–C(13)	155.0(1)
Ti–O(3)–C(25)	157.1(1)
Cl–Ti–O(1)	96.12(4)
Cl–Ti–O(2)	95.90(5)
Cl–Ti–O(3)	95.80(6)
Cl–Ti–O(4)	173.41(9)
O(1)–Ti–O(2)	118.95(6)
O(1)–Ti–O(3)	119.99(6)
O(1)–Ti–O(4)	79.72(9)
O(2)–Ti–O(3)	117.88(6)
O(2)–Ti–O(4)	81.83(9)
O(3)–Ti–O(4)	90.72(11)

[HOC$_6$H$_2$(CMe$_3$)$_2$-2,4-CH$_2$-6]$_3$N [structure (f), R = CMe$_3$], respectively, should give the "tied back" versions of complexes **2** and **6**.

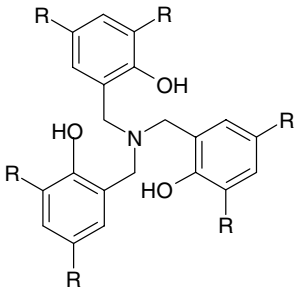

Structure (f) (R = Me, CMe$_3$)

Several alkoxo and phenoxo complexes of titanium containing these ligands have been reported [28–30]. In attempting to prepare chloro complexes, it was found that reactions of [TiCl$_4$] with either of these ligands in benzene in the presence of Et$_3$N gave mixtures which proved difficult to purify. This type of reaction is reported to give [TiCl{(OC$_6$H$_2$Me$_2$-2,4-CH$_2$-6)$_3$N}] in low yield but the complex has not been well characterised [31]. The complex was initially obtained via a circuitous route (Scheme 1).

We have noticed that when undried samples of (HOC$_6$H$_2$Me$_2$-2,4-CH$_2$-6)$_3$N, [(HOAr)$_3$N], are used in the reaction with [TiCl$_4$] and Et$_3$N, the oxo-bridged dimer [{N(ArO)$_3$}Ti–O–Ti{(OAr)$_3$N}]·1.5C$_6$H$_6$ (**10a**) is formed in good yield and this reacts with Me$_3$SiCl to give chloro complex **11**. There is an initial report of this dimer formed by the hydrolysis of [Ti(OCHMe$_2$){(OC$_6$H$_2$Me$_2$-2,4-CH$_2$-6)$_3$N}] in air [28] and the crystal structure of [{N(Ar′O)$_3$}Ti–O–Ti{(OAr′)$_3$N}]. [(OAr′)$_3$N = OC$_6$H$_2$-(CMe$_3$)$_2$-2,4-CH$_2$-6]$_3$N which is more resistant to hydrolysis has been obtained [30]. An X-ray crystal structure determination of the oxo-bridged dimer prepared in this work containing a pentane solvent molecule **10b** shows a distorted trigonal bipyramidal coordination geometry (Fig. 4) with bond lengths and angles (Table 4) which are similar to those found for the reported *tert*-butyl substituted analogue. The only significant difference between the two is the smaller Ti–O–Ti bond angle in **10b** [147.5(1)° cf. 155.5(1)°] which is apparently related to the smaller *ortho*-substituents providing less of a clash across the two sides of the molecule. In the *tert*-butyl substituted complex the *tert*-butyl groups are forced into close contact in the dimer with eight inter-titanium methyl–methyl contacts with C···C contacts shorter than the 4.0 Å sum of the van der Waals radii [30] but in **10b** there are no such close contacts.

[TiCl{(OC$_6$H$_2$Me$_2$-2,4-CH$_2$-6)$_3$N}] (**11**) was obtained more conveniently and in virtually quantitative yield by the reaction of the free ligand with [TiCl(OCHMe$_2$)$_3$] [18] prepared in diethyl ether from [TiCl$_4$] and 3 equivalents of [Ti(OCHMe$_2$)$_4$]. Complex **11** is not particularly soluble compared with the very soluble analogue [Ti(OCHMe$_2$){(OC$_6$H$_2$Me$_2$-2,4-CH$_2$-6)$_3$N}] [28]. The ^{1}H NMR spectrum shows a single set of resonances for the phenyl rings and the substituents while the benzylic CH protons form two very broad resonances. However, the ^{13}C{^{1}H}NMR spectrum shows only one CH$_2$ carbon resonance along with the other single set of carbon resonances. The *ipso*-carbon resonance appears at δ 160.2 which is upfield to that found for the non-tied-back analogue **2** (δ 164.4).

Addition of tris(3,5-di-*tert*-butyl-2-hydroxyphenyl)benzylamine to a diethyl ether solution of [TiCl(OCHMe$_2$)$_3$] gave the highly soluble complex [TiCl({OC$_6$H$_2$(CMe$_3$)$_2$-2,4-CH$_2$-6}$_3$N)]·diethyl ether (**12**) in virtually quantitative yield. The ^{1}H NMR spectrum showed a single set of resonances for the phenyl groups and the substituents and a well-defined AB spin system for the methylene protons. Although the structure has C_3-symmetry (see later for the X-ray structure) the methylene protons are non-equivalent due to the methylene carbon being pushed to one side in

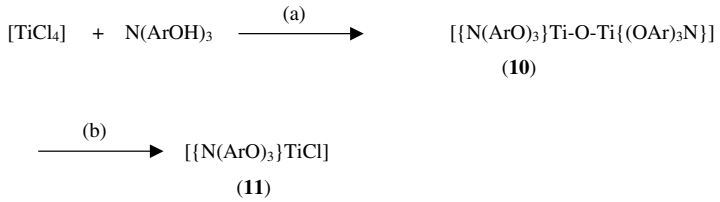

Scheme 1. (a) NEt$_3$ in benzene, reflux 14 h; (b) Me$_3$SiCl in toluene, stir 8 h.

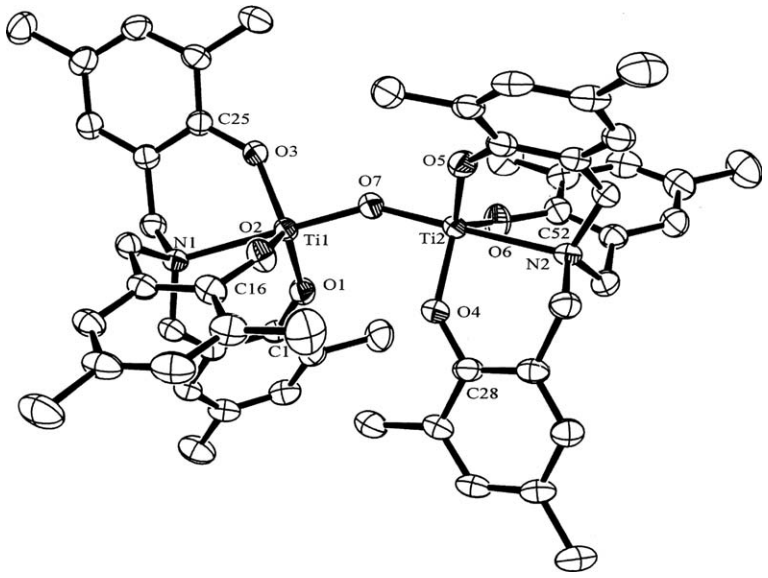

Fig. 4. ORTEP diagram of $[(Ti\{(OC_6H_2Me_2\text{-}2,4\text{-}CH_2\text{-}6)_3N\})_2O]\cdot n$-pentane (**10b**) showing the molecular structure. Hydrogen atoms are omitted for clarity. The *n*-pentane solvent molecule is not shown.

the six-membered ring. The AB system also indicates that rapid inversion of the structure does not occur on the NMR time scale [28]. In the $^{13}C\{^1H\}$ NMR spectrum there was a single set of resonances with the *ipso*-carbon resonances appearing at δ 160.8 which is similar to that found in methyl substituted complex **11** but lies upfield to the non-tied-back analogue 4-coordinate **6** (δ 164.4). An X-ray crystal structure of **12** showed a 5-coordinate distorted trigonal bipyramidal structure (Fig. 5a) in which the diethyl ether solvent molecule lies between the Ti complex molecules in the unit cell and is not coordinated. Bond lengths and angle are contained in Table 5.

The Ti–Cl bond [2.3074(7) Å] is similar to that found in the non-tied back trigonal bipyramidal $[TiCl(OC_6H_4Ph\text{-}2)_3\cdot(diethyl\ ether)]$ (**9**) [2.3067(6) Å] and both these bond lengths are longer than in tetrahedral $[TiCl\{OC_6H_3(CMe_3)_2 2,4\}_3]$ (**6**) [2.240(2) Å] which has a greater need for electron density at the metal. This electronic situation is further illustrated by the Ti–O bond lengths for the three molecules that are longer for the 5-coordinate complexes [ranges 1.809(2)–1.817(2) and 1.790(1)–1.794(1) Å for **12** and **9** cf. 1.756(2) Å for **6**]. In the trigonal bipyramidal complexes $[Ti(OCHMe_2)(\{OC_6H_2(CMe_3)_2\text{-}2,4\text{-}CH_2\text{-}6\}_3N)]$ [28] and $[Ti(OH)(\{OC_6H_2(CMe_3)_2\text{-}2,4\text{-}CH_2\text{-}6\}_3N)]$ [30] where there is an alkoxo or hydroxo ligand instead of Cl, the Ti–O bond lengths [ranges, respectively, 1.825(6)–1.866 Å and 1.783(2)–1.865(2) Å] are mostly longer than in **12** and **9** indicating that Cl is the poorer π-donor. This effect is also illustrated by comparison of the relative Ti–N bond lengths [2.216(2) Å in **12**; 2.334(5) and 2.364(2) Å, respectively, in the reported isopropoxo and hydroxo complexes] where the bond is shorter when N is trans to Cl. These features show there is a tightening of the Ti–O and Ti–N bonds when there is a less effective π-donor lying *trans* to the nitrogen atom.

In further comparisons of the relevant features of the coordination geometries for the complexes reported here, the O–Ti–Cl angles in the tied-back trigonal bipyramid (**12**) are similar to those in the non-tied-back trigonal bipyramid (**9**) [ranges 97.01(5)–97.18(5)° and 95.80(6)–96.12(4)°, respectively] as are the O–Ti–O bond angles [ranges 115.48(7)–120.72(7)° and 117.88(6)–119.99(6)°, respectively] showing that tying back has little effect on the trigonal bipyramidal geometry. However, for the tied-back trigonal bipyramidal geometry there is a significant effect for the Ti–O–C bond angles. In **12** the angles range from 143.5(2)° to 144.0(1)° whereas the angle widens in non-tied-back **9** [152.3(1)–157.1(1)°] (the complexes are expected to have similar electronic environments). In **6** where there is no tie-back constraint, the Ti–O–C bond angles are similar to those found for **9** [158.8(2)°]. There is obvious flexibility in this angle and this is even more pronounced in other complexes of this type of ligand. In the zwitterionic complex $[Zr\{(OC_6H_2Me_2\text{-}2,4\text{-}CH_2\text{-}6)_3NH\}_2]$ which has a low requirement for π-donation with six phenoxo ligands present and in which there is also room for a hydrogen atom on the inside of the cage at a non-agostic distance [2.688(3) Å], the angles range from 154(2)° to 160(2)° [32]. In $[W(O)(OCH_2CH_2OH)(\{OC_6H_2(CMe_3)_2\text{-}2,4\text{-}CH_2\text{-}6\}_3N)]$ where there is a similar low π-loading requirement for the phenoxo ligands the angles range from 126.0(2)–141.9(2)° [33]. For 1σ–2π donation from a phenoxo ligand, DFT calculations show there is a shallow minimum in the energy for the angle between about 160° and 180°, at 140° the energy is 20 kJ mol^{-1} and at 120° this energy rises to 60 kJ mol^{-1} [23].

Where the Ti–O–C bond angle is reduced it might be expected that the *tert*-butyl group would move away from the terminal Cl and create a wider but less well developed pocket about this ligand. However, inspection of the inter-

Table 4
Selected bond distances (Å) and angles (°) for [(Ti{($OC_6H_2Me_2$-2,4-CH_2-6)$_3$N})$_2$O] · *n*-pentane (**10b**)

Ti(1)–O(7)	1.8076(17)
Ti(1)–O(2)	1.8328(18)
Ti(1)–O(1)	1.8362(17)
Ti(1)–O(3)	1.8456(17)
Ti(1)–N(1)	2.379(2)
Ti(2)–O(7)	1.8219(17)
Ti(2)–O(5)	1.8304(18)
Ti(2)–O(4)	1.8348(18)
Ti(2)–O(6)	1.8387(19)
Ti(2)–N(2)	2.388(2)
O(1)–C(1)	1.357(3)
O(2)–C(16)	1.367(3)
O(3)–C(25)	1.355(3)
O(4)–C(28)	1.360(3)
O(5)–C(43)	1.360(3)
O(6)–C(52)	1.365(3)
O(7)–Ti(1)–O(2)	99.36(8)
O(7)–Ti(1)–O(1)	98.15(8)
O(2)–Ti(1)–O(1)	116.97(8)
O(7)–Ti(1)–O(3)	97.66(8)
O(2)–Ti(1)–O(3)	118.80(9)
O(1)–Ti(1)–O(3)	117.96(8)
O(7)–Ti(1)–N(1)	179.41(8)
O(2)–Ti(1)–N(1)	81.23(7)
O(1)–Ti(1)–N(1)	81.54(7)
O(3)–Ti(1)–N(1)	82.07(7)
O(7)–Ti(2)–O(5)	97.24(8)
O(7)–Ti(2)–O(4)	97.86(8)
O(5)–Ti(2)–O(4)	115.75(9)
O(7)–Ti(2)–O(6)	98.45(8)
O(5)–Ti(2)–O(6)	122.94(9)
O(4)–Ti(2)–O(6)	115.78(9)
O(7)–Ti(2)–N(2)	178.52(8)
O(5)–Ti(2)–N(2)	81.29(7)
O(4)–Ti(2)–N(2)	82.69(7)
O(6)–Ti(2)–N(2)	82.51(8)
C(1)–O(1)–Ti(1)	144.72(16)
C(16)–O(2)–Ti(1)	142.42(17)
C(25)–O(3)–Ti(1)	141.63(16)
C(28)–O(4)–Ti(2)	139.95(17)
C(43)–O(5)–Ti(2)	143.33(16)
C(52)–O(6)–Ti(2)	140.04(17)
Ti(1)–O(7)–Ti(2)	147.48(11)

atomic distances between the central *tert*-butyl group carbons and Cl in **6** and **12** shows that this effect is minimal on changing from the tetrahedral structure (C···Cl distance 4.87 Å) to the trigonal bipyramid (C···Cl distances 4.87, 4.91 and 4.93 Å). Noticeable in the two structures is that the titanium atom lies 0.60 Å above the plain made by the three phenoxide oxygen atoms in the tetrahedron but only 0.22 Å above them in the trigonal bipyramid. This is, of course, to be expected but it results in the chloro ligand lying 2.15 Å above the central carbon atoms of the three *tert*-butyl groups in the tetrahedron and 1.69, 1.78 and 1.85 Å in the trigonal bipyramid. The net effect is that when the methyl groups are taken into account, the trigonal bipyramidal structure creates a slightly better pocket about Cl than does the tetrahedron. The pocket structure in **12** is shown by the space-filling models in Fig. 5b and c.

Given the trigonal bipyramidal nature of complex **12** and the relevance of coordination expansion in the present studies, an excess of pyridine was added to the complex resulting in the formation of [(TiCl({$OC_6H_2(CMe_3)_2$-2,4-CH_2-6)$_3$N})(NC_5H_5)] (**13**). The ^{1}H NMR spectrum shows the methylene protons as a broadened singlet for this 6-coordinate compound compared with the AB quartet found for the 5-coordinate parent. The pyridine resonances in both the ^{1}H and ^{13}C{^{1}H} NMR spectra were very well-defined suggesting that fluxional processes are absent or are fast on the NMR timescale. Suitable crystals of the complex for X-ray crystallography have not yet been obtained but the structure is expected to be octahedral with the pyridine ligand coordinating *trans* to one of the phenoxo ligands. For this geometry the chloro ligand would still be surrounded by the *tert*-butyl groups but the pocket would be opened up on one side by the pyridine ligand. Recently, reported X-ray crystal structures show that this type of coordination geometry can be obtained from bidentate oxygen and nitrogen ligands [34].

3. Conclusion

The results of this work indicate that substituents in the *ortho*-position of the phenoxo ligand ring in tetrahedral chloro-tris-phenoxo complexes of titanium are positioned so as to create a coordination pocket or cavity about the chloro ligand. Where the substituent is a methyl group the effect is minimal but a *tert*-butyl substituent gives rise to a more substantial pocket. Coordination expansion can occur when a further donor ligand is available which removes this special environment. A phenyl substituent creates a better pocket but this can also be reduced in size when a further ligand binds creating a trigonal bipyramidal structure in which the pocket collapses somewhat. The collapse is due to the need to remove interactions of the phenoxo ligand phenyl ring with the ligand lying *trans* to the chloro ligand. Where an octahedral structure forms by filling two coordination sites, the possibility of isomers complicates the issue producing structures in which not all the *ortho*-substituents influence the chloro ligand. Where the collapse needs to be prevented, the tied-back ligand system gives rise to a trigonal bipyramidal structure of a more robust nature. A further ligand may coordinate leading to an octahedral structure which is expected to be more open on one side but it is obvious that the nature of this ligand is important given that diethyl ether does not coordinate but pyridine does. Overall it is apparent that *tert*-butyl groups in these complexes do not cover Cl completely forming what is best described as a steric pressure pocket [10d] whereas substituents that reach further outwards would form a more enclosed pocket or cavity. Given the availability of a wide variety of phenol ligands substituted in the *ortho*-position, the chloro-tris-phenoxo approach to the molecular engineering of coordination pockets should have future potential. By varying the size of the substituent,

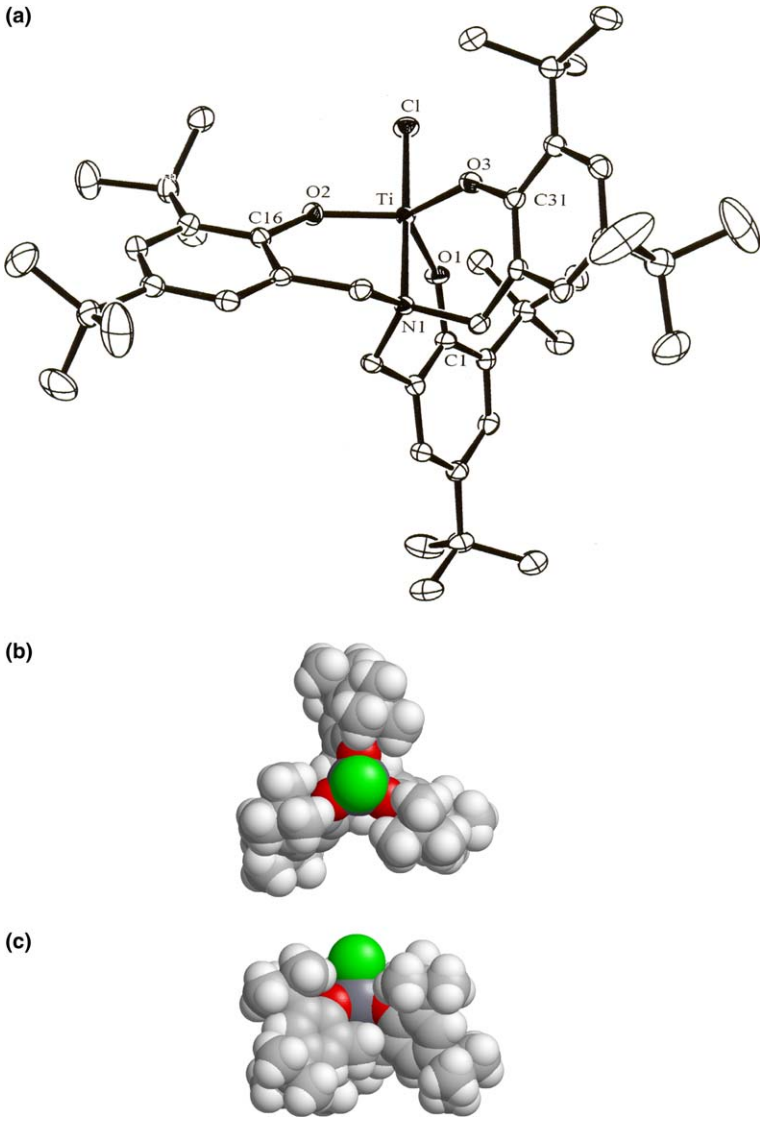

Fig. 5. (a) ORTEP diagram of $[TiCl(\{OC_6H_2(CMe_3)_2\text{-}2,4\text{-}CH_2\text{-}6\}_3N)]\cdot$ diethyl ether (**12**) showing the molecular structure. Hydrogen atoms have been removed for clarity. The diethyl ether solvent is not shown. (b) Space-filling model looking down the Cl–Ti bond showing the pocket arrangement about Cl. (c) Space-filling model, side-on view of the Ti–Cl bond showing the extent to which the *tert*-butyl group methyls cover the Cl atom.

collapsible through to non-collapsible complexes with different pocket characteristics may be realised.

4. Experimental

4.1. General methods and materials

All preparations and manipulations were carried out under dry oxygen-free nitrogen using standard bench-top techniques for air-sensitive substances. $[TiCl_4]$ and the phenols were used as received from commercial sources. 4,4′-Dimethyl-2,2′-bibyridyl (dmbipy) was dried under vacuum before use. Tris(2-hydroxy-4,6-di-*tert*-butylbenzyl)amine and tris(2-hydroxy-4,6-dimethylbenzyl)amine were prepared by the literature procedures [28]. Light petroleum (b.p. 40–60 °C) and toluene were distilled from sodium wire and dichloromethane from freshly ground CaH_2. ^1H and $^{13}C\{^1H\}$ NMR spectra were recorded at 400 and 100 MHz, respectively, on a Bruker AM400 spectrometer. $CDCl_3$ and CD_2Cl_2 were dried over, and distilled from, freshly ground CaH_2 and benzene-d_6 from sodium wire. C, H and N analyses were determined by Dr. A. Cunninghame and associates, University of Otago, New Zealand. The production of HCl gas in the thermalisation reactions was monitored by passing the exhaust gases from the nitrogen bubbler over *N*,*N*,*N*′,*N*′-tetramethylethylenediamine and observing the white cloud produced.

4.2. Synthesis

4.2.1. $[TiCl(OC_6H_4CMe_3)_3\text{-}4]\cdot 0.5C_7H_8$ (**1**)

4-*tert*-Butylphenol (4.75 g, 31.6 mmol) in toluene (40 cm^3) was added to $[TiCl_4]$ (2.0 g, 10.5 mmol) in toluene (40 cm^3) and the mixture was refluxed until no more HCl

Table 5
Selected bond distances (Å) and angles (°) for [TiCl({$OC_6H_2(CMe_3)_2$-2,4-CH_2-6}$_3$N)]·(OEt_2) (**12**)

Ti–O1	1.809(2)
Ti–O2	1.817(2)
Ti–O3	1.811(2)
Ti–N1	2.216(2)
Ti–Cl	2.3074(7)
O1–C1	1.363(3)
O2–C16	1.370(3)
O3–C31	1.367(3)
N1–C7	1.501(3)
N1–C22	1.495(3)
N1–C37	1.497(3)
O(1)–Ti–O(2)	119.29(7)
O(1)–Ti–O(3)	115.48(7)
O(3)–Ti–O(2)	120.72(7)
O(1)–Ti–N(1)	82.76(7)
O(2)–Ti–N(1)	82.66(7)
O(3)–Ti–N(1)	83.30(7)
O(1)–Ti–Cl(2)	97.10(5)
O(3)–Ti–Cl(2)	97.18(5)
O(2)–Ti–Cl(2)	97.01(5)
N(1)–Ti–Cl(2)	179.51(5)
C(1)–O(1)–Ti	143.54(15)
C(16)–O(2)–Ti	143.66(14)
C(31)–O(3)–Ti	143.97(14)

gas was produced (12 h). NMR spectroscopy at this stage confirmed that no 4-*tert*-butylphenol was present. The cooled solution was filtered, the solvent was removed and the residue held under vacuum for 2 h giving the complex as a deep-red flaky solid. Yield: 5.82 g, 97%. *Anal*. Calc. for $C_{33.5}H_{43}ClO_3Ti$: C, 69.73; H, 7.51. Found: C, 69.48; H, 7.58%. ^{1}H NMR: δ 1.27 (s, 27H, CMe_3), 2.40 [s, 1.5H, 0.5CH_3(toluene)], 7.11 (b, 12H, *o* and *m*-Hs), 7.22 and 7.30 (m, 2.5H, 0.5 aromatics (toluene). ^{13}C{^{1}H} NMR: δ 21.5 [Me(toluene)], 31.5 (CMe_3), 34.2 (C), 118.7 (b, *o*-C) 124.7 (toluene), 124.6 (b, *m*-C), 128.2 (toluene), 129.0 (toluene), 137.9 [*ipso*-C(toluene)], 145.8 (b, C), 164.6 (*ipso*-C).

4.2.2. [{TiCl($OC_6H_3Me_2$-2,4)$_2$(μ-$OC_6H_3Me_2$-2,4)}$_2$] (**2**)

2,4-Dimethylphenol (3.87 g, 31.7 mmol) in toluene (40 cm^3) was added to [$TiCl_4$] (2.0 g, 10.5 mmol) in toluene (40 cm^3) and the mixture was refluxed until no more HCl gas was produced (12 h). The cooled solution was filtered, the solvent was removed and the residue held under vacuum for 2 h giving a gum that formed the complex as a deep-red crystalline mass on standing overnight. Yield: 4.5 g, 96%. *Anal*. Calc. for $C_{24}H_{27}ClO_3Ti$: C, 64.51; H, 6.09. ^{1}H NMR: δ (s, 9H, Me), 2.20 (s, 9H, Me), 6.72–6.89 (m, 9H, *o* and *m*-Hs). ^{13}C{^{1}H} NMR: δ 16.6 (Me), 20.7 (Me), 119.5 (CH), 126.3 (C), 126.9 (CH), 131.0 (CH), 133.2 (C), 164.4 (*ipso*-C). Crystalline material was cut from the mass and used for the X-ray analysis.

4.2.3. [TiCl($OC_6H_3Me_2$-2,4)$_3$(dmbipy)] (**3**)

4,4′-Dimethyl-2,2′-bipyridine (0.4 g, 2.17 mmol) in CH_2Cl_2 (20 cm^3) was added to complex **2** (0.96 g, 2.15 mmol) in CH_2Cl_2 (20 cm^3) and the mixture was stirred for 1 h. The solution was filtered and the solvent removed to give the complex as an orange flaky solid. Yield: 1.30 g, 96%. *Anal*. Calc. for $C_{36}H_{39}ClN_2O_3Ti$: C, 68.52; H, 6.23, N, 4.44. Found: C, 67.80; H, 6.73, N, 4.68%. ^{1}H NMR: δ 1.67 (s, 3H, Me); 2.06 (s, 3H, Me); 2.24 (s, 6H, 2Me); 2.34 (s, 6H, 2Me); 2.40 (s, 6H, 2Me); 6.25 [d, ^3J(HH) 8.1, 1H, *o*-H]; 6.46 [dd, ^3J(HH) 8.1, ^4J(HH) 1.6, 1H, *m*-H]; 6.58 [d, ^4J(HH) 1.6, 1H, *m*-H]; 6.83 [dd, ^3J(HH) 8.1, ^4J(HH) 1.5, 2H, *m*-Hs]; 6.91 [d, ^4J(HH) 1.5, 2H, *m*-Hs]; 7.20 [d, ^3J(HH) 5.5, 2H, *m*-H dmbipy]; 7.38 [d, ^3J(HH) 8.1, 2H, *o*-Hs]; 7.81 [bd, 2H, *m*-Hs dmbipy]; 8.95 [d, ^3J(HH) 5.5, 2H, *o*-Hs dmbipy]. ^{13}C{^{1}H} NMR: δ 16.1 (1Me); 17.1 (2Me); 20.4 (1Me); 20.7 (2Me); 21.5 (2Me, dmbipy); 118.5 (1CH); 120.1 (2CH); 122.2 (*m*-CH, dmbipy); 126.3 (2C); 126.4 (1*m*-CH); 126.6 (2*m*-CHs, dmbipy); 127.0 (2*m*-CHs); 128.7 (1C); 128.9 (1C); 130.1 (2C); 130.3 (1*m*-CH); 130.7 (2*m*-CHs); 149.0 (2*o*-CHs, dmbipy); 150.7 (2Cs, dmbipy); 151.7 (2Cs, dmbipy); 162.7 (1 *ipso*-C); 163.51 (2 *ipso*-Cs).

4.2.4. [TiCl($OC_6H_2Me_3$-2,4,6)$_3$] (**4**)

2,4,6-Trimethylphenol (4.31 g, 31.7 mmol) in toluene (40 cm^3) was added to [$TiCl_4$] (2.0 g, 10.5 mmol) in toluene (40 cm^3) and the mixture was refluxed until no more HCl gas was produced (15.5 h). The cooled solution was filtered from a small amount of solid, the solvent was removed and the residue held under vacuum for 2 h giving a gum which formed the complex as a deep-red crystalline mass on standing overnight. Yield: 4.5 g, 87%. *Anal*. Calc. for $C_{27}H_{33}ClO_3Ti$: C, 66.33; H, 6.80. Found: C, 65.88; H, 6.70%. ^{1}H NMR: δ 2.19 (s, 9H, Me), 2.26 (bs, 18H, Me), 6.72 (bs, 6H, *m*-Hs). ^{13}C{^{1}H} NMR: δ 16.9 (*o*-Me), 20.6 (*p*-Me), 126.7 (*o*-C), 128.6 (CH), 132.4 (*p*-C), 163.9 (*ipso*-C).

4.2.5. [TiCl{$OC_6H_3(CHMe_2)_2$-2,6}$_3$] (**5**)

2,6-Di-*iso*-propylphenol (3.0 g, 16.8 mmol) in toluene (30 cm^3) was added to [$TiCl_4$] (1.0 g, 5.27 mmol) in toluene (30 cm^3) and the mixture was refluxed until no more HCl gas was produced (19.5 h). The cooled solution was filtered and the solvent removed giving an orange solid. NMR spectroscopy at this stage indicated the presence of unreacted phenol and two coordination products. The crude material was dissolved in toluene (50 cm^3), the volume reduced to ca. 30 cm^3 and the solution stood at −20 °C, giving the complex as a non-crystalline orange solid containing several large crystals of [Ti{$OC_6H_3(CHMe_2)_2$-2,6}$_4$] which were manually removed from the product. Yield: 1.30 g, 40%. *Anal*. Calc. for $C_{36}H_{51}ClO_3Ti$: C, 70.29; H, 8.36. Found: C, 70.78; H, 8.88%. ^{1}H NMR: δ 1.13 [d, ^3J(HH) 6.9, 36H, CMe_2], 3.42 [sept, ^3J(HH) 6.9, CH], 6.91 (t, 3H, *p*-Hs), 7.03 (m, 6H, *m*-Hs). ^{13}C{^{1}H} NMR: δ 23.2 (Me), 27.5 (CH), 123.0 (*m*-C), 123.8 (*p*-C), 137.4 (*o*-C), 163.1 (*ipso*-C). The NMR spectra are identical to that found for the complex prepared in refluxing benzene [20,21].

*4.2.6. [TiCl{$OC_6H_3(CMe_3)_2$-2,4}$_3$] (**6**)*

Method A: 2,4-Di-*tert*-butylphenol (9.8 g, 47.5 mmol) in toluene (60 cm^3) was added to [$TiCl_4$] (3.0 g, 15.8 mmol) in toluene (50 cm^3) and the mixture was refluxed until no more HCl gas was produced (14.5 h). After refluxing for a further 2 h, the cooled solution was filtered and the solvent removed giving a crystalline orange-red solid. Crude yield: 11.0 g, 99%. This material has a slight red tinge and NMR spectroscopy indicated the presence of a small amount of unreacted phenol (ca. 3–5%) but it was sufficiently pure for further use. The solid was washed with petroleum spirit (40 cm^3) giving the complex as an orange crystalline solid. Yield: 9.21 g, 83%. (Further complex can be obtained by cooling the petroleum spirit washings.) *Anal*. Calc. for $C_{42}H_{63}ClO_3Ti$: C, 72.13; H, 9.08. Found: C, 71.96; H, 9.26%. ^{1}H NMR: δ 1.29 (s, 27H, CMe_3), 1.46 (s, 27H, CMe_3), 7.10 (s, 6H, *o* and *m*-Hs), 7.29 [d, ^4J(HH) 1.3, 3H, *m*-H). $^{13}C\{^1H\}$ NMR: δ 30.3 (Me), 31.6 (Me), 34.6 (C), 35.1 (C), 122.7 (CH), 123.4 (CH), 124.0 (CH), 135.6 (C), 146.3 (C), 163.2 (*ipso*-C). On a larger scale, a reaction between 26.15 g of 2,4-di-*tert*-butylphenol (0.127 mol) and 8 g of [$TiCl_4$] (0.0422 mol) in 120 cm^3 of toluene produced 28.5 g (97%) of the crude product after refluxing for 21 h.

Method B: *n*-Butyl lithium (9.8 cm^3 of a 1.6 mol L^{-1} solution, 15.8 mmol) in hexane was added dropwise to a solution of 2,4-di-*tert*-butylphenol (3.26 g, 15.8 mmol) in diethyl ether (50 cm^3) cooled to −30°C and the solution was stirred with the cooling bath removed for 2 h. [$TiCl_4$] (1.0 g, 5.27 mmol) was added to a flask which was then cooled to −78 °C and diethyl ether (50 cm^3) was added. The solution was heated until all the yellow solid dissolved and then recooled to −78 °C and the lithium phenoxide solution added via a cannula. The cooling bath was removed and the solution stirred for 20 h, filtered and the solvent removed to give the crude complex as an orange crystalline solid (yield: 3.08 g) which was dissolved in diethyl ether (50 cm^3). The solution was filtered and the volume reduced to ca. 25 cm^3 giving the complex as yellow-orange crystals on standing. Yield: 1.24 g, 34%. *Anal*. Calc. for $C_{42}H_{63}ClO_3Ti$: C, 72.13; H, 9.08. Found: C, 72.14; H, 8.72%. The complex has identical NMR spectra to the sample prepared under method A. A single crystal from the mass was used for the X-ray analysis.

4.2.7. [TiCl{$OC_6H_3(CMe_3)_2$-2,4}$_3$(dmbipy)] (7)

4,4′-Dimethyl-2,2′-bipyridine (0.267 g, 1.45 mmol) in CH_2Cl_2 (20 cm^3) was added to complex **6** (1.014 g, 1.45 mmol) in CH_2Cl_2 (20 cm^3) and the mixture was stirred for 2 h. The solution was filtered and the solvent removed to give the complex as an orange flaky solid. Yield: 1.28 g, 99%. *Anal*. Calc. for $C_{54}H_{75}ClN_2O_3Ti$: C, 73.40; H, 5.56, N, 3.17. Found: C, 73.04; H, 5.76, N, 3.09%. The NMR spectra are very complicated due to the presence of isomers. Only the ^{1}H NMR of the distinguishable major isomer is reported: δ 1.28 (s, 18H, $2CMe_3$); 1.31 (s, 9H, CMe_3); 1.37 (s, 18H, $2CMe_3$); 1.51 (s, 9H, CMe_3); 2.31 (s, 6H, 2Me dmbipy); 6.96 [dd, ^3J(HH) 8.2, ^4J(HH) 2.4, 2H, *m*-Hs]; 6.98 (obscured dd, 1H, *m*-H); 7.09 [d, ^3J(HH) 5.6, 2H, *m*-Hs dmbipy]; 7.11 [d, ^3J(HH) 8.4, ^4J(HH) 2.3, 1H, *m*-H]; 7.23 [d, ^4J(HH) 2.4, 2H, *m*-Hs]; 7.29 [d, J(HH) 2.3, 1H, *m*-H]; 7.55 [bd, ^3J(HH) 8.2, 2H, *o*-Hs]; 7.91 (s, 2H, *m*-Hs dmbipy); 8.93 [d, ^3J(HH) 5.6, 2H, *o*-Hs dmbipy]. Easily distinguishable *ortho*-hydrogen resonances for the other isomers are at δ 8.79 and 8.53.

*4.2.8. [TiCl(OC_6H_4Ph-2)$_3$] (**8**)*

2-Hydroxybiphenyl (8.1 g, 47.6 mmol) in dichloromethane (50 cm^3) was added to [$TiCl_4$] (3.0 g, 15.8 mmol) in dichloromethane (50 cm^3) and the mixture was refluxed until no more HCl gas was produced (30 h). The cooled solution was filtered, the solvent was removed giving a dark red gum which failed to solidify on extended pumping. The complex was identified on the basis of NMR spectral characteristics that were similar to complex **9**. ^{1}H NMR: δ 6.58 [d, ^3J(HH) 7.4, 3H, *o*-H], 7.01 [t, ^3J(HH) 7.4, 3H, *p*-H], 7.07 [t, ^3J(HH) 7.4, 3H, *m*-H], 7.12–7.18 [m, 9H, *m* and *p*-Hs(phenyl substituent)], 7.20 [dd, ^3J(HH) 7.4, ^4J(HH) 1.4, 3H, *m*-H], 7.32 [d, ^3J(HH) 7.4, 6H, *o*-Hs(phenyl substituent)]. $^{13}C\{^1H\}$ NMR: δ 120.4 (CH), 124.0 (CH), 127.3 (CH), 128.2 (CH), 128.3 (CH), 129.2 (CH), 130.0 (CH), 130.6 (C), 137.3 (C), 163.6 (*ipso*-C).

*4.2.9. [TiCl(OC_6H_4Ph-2)$_3$(diethyl ether)] (**9**)*

n-Butyl lithium (15.3 cm^3 of a 1.6 mol L^{-1} solution, 24.4 mmol) in hexane was added dropwise to a solution of 2-hydroxybiphenyl (4.15 g, 24.4 mmol) in diethyl ether (80 cm^3) cooled to −30°C and the solution was stirred with the cooling bath removed for 2 h. [$TiCl_4$] (1.54 g, 8.1 mmol) was added to a flask which was then cooled to −78 °C and diethyl ether (80 cm^3) was added. The solution was heated until all the yellow solid dissolved and after cooling to room temperature, it was added via a cannula to the suspension of the lithium phenoxide cooled to −78 °C. The cooling bath was removed and the solution stirred for 20 h, filtered and the remaining solid washed with diethyl ether until it was no longer coloured orange. The combined filtrate and washings were kept hot while the volume was reduced to approximately half and on standing the complex formed as large ruby-red crystals. Yield: 1.8 g, 51%. *Anal*. Calc. for $C_{40}H_{37}ClO_4Ti$: C, 72.24; H, 5.61. Found: C, 71.91; H, 5.48%. ^{1}H NMR: δ 1.13 [t, ^3J(HH) 7.0, 6H, Me], 3.45 [q, ^3J(HH) 7.0, 4H, CH_2], 6.62 (d, 3H, aromatic-H), 6.99 (t, 3H, aromatic-H), 7.05 (t, 3H, aromatic-H), 7.09–7.20 (m, 12H, aromatic-Hs), 7.32 (d, 6H, aromatic-Hs). $^{13}C\{^1H\}$ NMR: δ 15.0 (Me), 66.0 (CH_2), 120.5 (CH), 123.6 (CH), 127.2 (CH), 128.2 (CH), 129.2 (CH), 130.0 (CH), 130.3 (C), 137.5 (*o*-C),163.2 (*ipso*-C). A single crystal from the mass was used for the X-ray analysis.

*4.2.10. [(Ti{($OC_6H_2Me_2$-2,4-CH_2-6)$_3$N})$_2$O] · 1.5C_6H_6 (**10a**)*

Undried tris(2-hydroxy-4,6-dimethylbenzyl)amine (1.77 g, 4.22 mmol) in benzene (40 cm^3) was added dropwise to

a stirred solution of [$TiCl_4$] (0.8 g, 4.28 mmol) in benzene (40 cm^3) and triethylamine (1.8 cm^3, 12.74 mmol) was added dropwise. The mixture was refluxed for 14 h, the cooled solution filtered and the solvent removed to give the complex as yellow crystalline solid which was washed with chilled diethyl ether (30 cm^3). Yield: 2.0 g, 100%. *Anal.* Calc. for $C_{54}H_{60}N_2O_7Ti_2 \cdot 1.5C_6H_6$: C, 71.25; H, 6.55; N, 2.64. Found: C, 71.39; H, 6.76; N, 2.90%. ^{1}H NMR: δ (C_6D_6) 2.15 (s, 9H, Me), 2.38 (s, 9H, Me), 2.8 (b, 3H, CH), 3.8 (b, 3H, CH), 6.54 (bs, 3H, *m*-CH), 6.73 (bs, 3H, *m*-CH), 7.28 (benzene). ^{13}C{^{1}H} NMR: δ 16.1 (Me), 20.7 (Me), 58.8 (CH_2),124.3 (C), 125.0 (C), 128.5 (CH), 129.3 (C), 131.0 (CH), 160.8 (*ipso*-C). A single crystal obtained from the mass produced on recrystallisation from *n*-pentane was used for the X-ray analysis [complex **10b**].

4.2.11. [TiCl{($OC_6H_2Me_2$-2,4-CH_2-6)$_3$N}] (**11**)

Method A: Chlorotrimethylsilane (2 cm^3, 1.34 mmol) was added via a syringe to [(Ti{($OC_6H_2Me_2$-2,4-CH_2-6)$_3$N})$_2$O] (0.6 g, 0.67 mmol) in toluene (30 cm^3) and the mixture was stirred for 8 h. The solution was filtered and the orange precipitate dried under vacuum. Yield: 0.49 g, 73%. *Anal.* Calc. for $C_{27}H_{30}ClNO_3Ti$: C, 64.87; H, 6.05, N, 2.80. Found: C, 64.82; H, 6.32; N, 2.97%. ^{1}H NMR (the complex is only slightly soluble in $CDCl_3$): δ 2.22 (s, 9H, Me), 2.25 (s, 9H, Me), 2.9 (b, 3H, CH), 3.9 (b, 3H, CH), 6.73 (bs, 3H, *m*-H), 6.88 (bs, 3H, *m*-H). ^{13}C{^{1}H} NMR: δ 15.8 (Me), 20.7 (Me), 58.5 (CH_2), 122.8 (C), 124.4 (C), 127.2 (CH), 131.1 (CH), 131.3 (C), 160.2 (*ipso*-C).

Method B: [$TiCl_4$] (0.29 g, 1.52 mmol) was cooled to −78 °C and diethyl ether (40 cm^3) was added. The solution was heated to dissolve the yellow solid, cooled to room temperature and added dropwise to [$Ti(OCHMe_2)_4$] (1.30 g, 4.57 mmol) in diethyl ether (30 cm^3). The mixture was stirred for 30 min [$TiCl(OCHMe_2)_3$] equivalent: (1.59 g, 6.08 mmol) and dry tris(2-hydroxy-4,6-dimethylbenzyl)amine (2.55 g, 6.08 mmol) in diethyl ether (40 cm^3) added dropwise. The mixture was stirred for 2 h and the orange precipitate filtered off and dried under vacuum. Yield: 2.92 g, 96%. *Anal.* Calc. for $C_{27}H_{30}ClNO_3Ti$: C, 64.87; H, 6.05, N, 2.80. Found: C, 65.31; H, 6.41; N, 2.81%. The complex had similar NMR spectra to the sample prepared under method A.

4.2.12. [TiCl({$OC_6H_2(CMe_3)_2$-2,4-CH_2-6}$_3$N)] · diethyl ether (**12**)

[$TiCl_4$] (0.234 g, 1.23 mmol) was cooled to −78 °C and diethyl ether (40 cm^3) was added. The solution was heated to dissolve the yellow solid, cooled to room temperature and added dropwise to [$Ti(OCHMe_2)_4$] (1.05 g, 3.69 mmol) in diethyl ether (30 cm^3). The mixture was stirred for 30 min ([$TiCl(OCHMe_2)_3$] equivalent: 1.286 g, 4.95 mmol) and dry tris(2-hydroxy-4,6-di-*tert*-butylbenzyl)amine (3.33 g, 4.96 mmol) in diethyl ether (40 cm^3) added dropwise. The mixture was stirred for 2 h, the solution filtered and the solvent removed to give an orange crystalline solid. Yield: 2.92 g, 96%. *Anal.* Calc. for $C_{45}H_{66}ClNO_3Ti$ (i.e., [{$N(ArO)_3$}TiCl]): C, 71.81; H, 8.84, N, 1.86. Found: C, 72.99; H, 8.76; N, 2.01%. The solid was dissolved in diethyl ether (120 cm^3) and the solvent kept hot and removed in vacuo until crystallisation could no longer be prevented. On standing, well formed orange crystals were formed. Further crystalline product was obtained by repeating this process. *Anal.* Calc. for $C_{49}H_{76}ClNO_4Ti$: C, 71.21; H, 9.27; N, 1.70. Found: C, 71.45; H, 9.36; N, 1.69%. ^{1}H NMR: δ 1.26 (t, 6H, diethyl ether),1.34 (s, 27H, CMe_3), 1.52 (s, 27H, CMe_3), 3.18 [d, ^2J(AB) 13.9, 3H, CH], 3.53 [d, ^2J(AB) 13.9, 3H, CH], 7.09 [d, ^3J(HH) 2.1, 3H, *m*-H], 7.31 [d, ^3J(HH) 2.1, 3H, *m*-H]. ^{13}C{^{1}H} NMR: δ 15.3 (Me, diethyl ether), 29.6 (CMe_3), 31.6 (CMe_3), 34.5 (C), 34.9 (C), 58.7 (CH_2), 65.8 (CH_2,diethyl ether), 123.3 (*o*-C), 123.5 (*m*-CH), 124.0 (*m*-CH), 135.7 (*p*-C), 144.3 (*o*-C), 160.8 (*ipso*-C). A single crystal from the mass was used for the X-ray analysis.

4.2.13. [TiCl{($OC_6H_2(CMe_3)_2$-2,4-CH_2-6)$_3$N}(NC_5H_5)] (**13**)

Pyridine (0.2 g, 2.5 mmol) in diethyl ether (10 cm^3) was added dropwise from a syringe to a rapidly stirred solution of complex **12** (0.373 g, 0.45 mmol) in diethyl ether and the mixture was stirred for 2 h. The solution was filtered and the brown microcrystalline solid dried in vacuo. Yield: 0.364 g, 97%. *Anal.* Calc. for $C_{50}H_{71}ClN_2O_3Ti$: C, 72.23; H, 8.61; N, 3.44. Found: C, 72.70; H, 9.27; N, 3.66%. ^{1}H NMR (CD_2Cl_2): δ 1.99 (t, 6H, Me), 1.32 (s, 27H, CMe_3), 1.49 (s, 27H, CMe_3), 3.47 (q, 4H, CH_2), 3.64 (bs, 6H, CH_2), 7.09 [d, ^3J(*HH*) 2.2, 3H, *m*-H], 7.31 [d, ^3J(*HH*) 2.2, 3H, *m*-H], 7.31–7.35 (obsm, 2H, *m*-H_{py}), 7.73 (td, ^3J(*HH*) 7.7, 1H, (*p*-H_{py})), 8.63 (bs, 2H, *o*-H_{py}). ^{13}C{^{1}H} NMR: δ 15.5 ($Me_{diethyl\ ether}$), 29.7 (CMe_3), 31.7 (CMe_3), 34.8 (C), 35.2(C), 59.0 (CH_2), 66.1 ($CH_{2diethyl\ ether}$), 123.9 (CH), 123.95 (*o*-C), 124.2 (*m*-CH_{py}), 135.8 (*p*-C), 136.4 (*p*-CH_{py}),144.8 (*o*-C), 150.1 (*o*-CH_{py}), 161.1 (*ipso*-C).

4.3. X-ray crystallography

Crystallographic and refinement data are given in Table 6. Data collected, with graphite monchromated Mo Kα X-radiation, were measured on a Siemens SMART CCD area detector diffractometer with the omega scan method. The data were corrected for Lorentz and polarisation effects and for absorption by the multi-scan method [35]. The structures were solved by direct methods [36] and refined by full-matrix least-squares methods [37] on F^2. Hydrogen atoms were placed in calculated positions and were refined with a riding model ($U_{iso} = 0.08$). Diagrams were prepared by ORTEP [38] and RASTOP [39]. Selected bond distances and angles are listed in Tables 1–5. Complex **2** is dimeric lying across a centre of symmetry. Some disorder was noted for the Cl (with a site occupancy ratio of ca. 90:10) and also for the H atoms in the Me group in the 4 positions of both terminal phenoxo ligands. The occupancies of these latter were fixed at 0.5. In **6** the *tert*-butyl group in the para

Table 6
Crystallographic data and structural information

Compound	**2**	**6**	**9**	**10b**	**12**
Molecular formula	$C_{24}H_{27}ClO_3Ti$	$C_{42}H_{63}ClO_3Ti$	$C_{40}H_{37}ClO_4Ti$	$C_{39}H_{72}N_2O_7Ti_2$	$C_{40}H_{37}ClNO_4Ti$
M_r	446.81	699.27	665.05	1016.99	826.46
T (K)	150(2)	293(2)	150(2)	150(2)	189(2)
Crystal size (mm)	$0.40 \times 0.30 \times 01.6$	$0.22 \times 0.24 \times 0.38$	$0.50 \times 0.40 \times 0.40$	$0.42 \times 0.30 \times 0.22$	$0.38 \times 0.18 \times 0.18$
Crystal system	monoclinic	hexagonal	monoclinic	triclinic	monoclinic
Space group	$P2_1/c$	$R\bar{3}$	$P2_1/n$	$P\bar{1}$	$P2_1/n$
a (Å)	10.9316(1)	16.680(2)	13.1474(2)	12.3309(2)	15.0358(3)
b (Å)	25.7193(1)	16.680(2)	17.3038(2)	12.9833(2)	15.8104(2)
c (Å)	8.0853(1)	27.248(5)	15.3222(2)	20.0930(2)	20.6045(4)
α (°)	90.0	90.0	90.0	84.258(1)	90.0
β (°)	93.882(1)	90.0	94.725(1)	72.168(1)	92.630(1)
γ (°)	90.0	120.0	90.0	66.649(1)	90.0
V (Å^3)	2267.99(4)	6565.3(16)	3473.95(8)	2810.61(7)	4892.98(15)
Z	4	6	4	2	4
D_{calc} (mg cm^{-3})	1.309	1.061	1.272	1.202	1.122
μ (mm^{-1})	0.516	0.289	0.363	0.335	0.270
F (000)	936	2268	1392	1080	1792
θ Range for data collection (°)	1.58–23.32	1.60–25.00	1.78–26.30	1.06–25.35	1.62 to 26.43
Reflections collected	10347	11450	19986	24227	28138
Unique reflections (R_{int})	3267 (0.0172)	2582 (0.0242)	7008 (0.0193)	10220 (0.0252)	10004 (0.0440)
Reflections with [$I > 2\sigma(I)$]	2983	2203	5712	8045	7179
Refined parameters	275	173	443	647	526
Completeness to $\theta = x°$ (%)	23.32, 99.8	25.0, 100.0	26.30, 99.3	25.35, 99.2	26.43, 99.3
Absorption correction T_{max}, T_{min}	0.922, 0.820	0.939, 0.898	0.869, 0.839	0.930, 0.872	0.953, 0.905
Goodness-of-fit (all data)	1.045	1.124	1.056	1.051	1.051
Final R indices [$I > 2\sigma(I)$] (R_1,wR_2)	0.0303, 0.0824	0.0613, 0.1895	0.0357, 0.0891	0.0451, 0.1143	0.0496, 0.1035
R indices (all data) (R_1, wR_2)	0.0338, 0.0843	0.0699, 0.1961	0.0492, 0.0974	0.0632, 0.1287	0.0833, 0.1204
Maximum, minimum $\Delta\rho$ (e Å^{-3})	0.396, −0.374	0.658, −0.576	0.240, −0.373	0.511, −0.437	0.533, −0.419

position is disordered (ratio ca. 80:20) and in **9** two sites (ratio 65:35) have been distinguished for the co-ordinated ether molecule. Solvent of crystallisation was present in **10b** (*n*-pentane) and **12** (ether).

5. Supplementary data

CCDC 281293–281297 contains the supplementary crystallographic data for this paper. These data can be obtained free of charge from The Cambridge Crystallographic Data Centre via www.ccdc.cam.ac.uk/datarequest/cif.

References

[1] N. Kitajima, W.B. Tolman, Prog. Inorg. Chem. (1995) 419.
[2] S.R. Colinson, D.A. Fenton, Coord. Chem. Rev. 148 (1996) 19.
[3] G. Parkin, Chem. Rev. 104 (2004) 702.
[4] B. Kersting, Z. Anorg. Allg. Chem. 630 (2004) 765.
[5] A.R. van Doorn, M. Bos, S. Harkema, J. van Eerden, W. Verboom, D.N. Reinhoudt, J. Org. Chem. 56 (1991) 2371.
[6] V. van Axel-Castelli, A. Dalla-Cort, L. Mandolini, D.N. Reinhoudt, L. Schiaffino, Chem. Eur. J. 6 (2000) 1193.
[7] V. van Axel-Castelli, A. Dalla-Cort, L. Mandolini, V. Pinto, D.N. Reinhoudt, F. Ribaudo, C. Sanna, L. Schiaffino, B.H.M. Snellinkruel, Supramol. Chem. 14 (2002) 211.
[8] R.R. Conry, G. Ji, A.A. Tipton, Inorg. Chem. 38 (1999) 906.
[9] B.S. Hammes, D. Ramos-Maldonado, G.P.A. Yap, L. Liable-Sands, A.L. Rheingold, V.G. Young Jr., A.S. Borovik, Inorg. Chem. 36 (1997) 3210.
[10] (a) For recent work related to reduction of ammonia see: D.V. Yandulov, R.R. Schrock, Can. J. Chem. 83 (2005) 341;
(b) D.V. Yandulov, R.R. Schrock, Inorg. Chem. 44 (2005) 1103;
(c) V. Ritleng, D.V. Yandulov, W.W. Weare, R.R. Schrock, A.S. Hock, W.M. Davis, J. Am. Chem. Soc. 126 (2004) 6150;
(d) For general work related to this ligand type see: R.R. Schrock, Acc. Chem. Res. 30 (1997) 9.
[11] (a) For titanium see: J.C. Peters, A.R. Johnson, A.L. Odom, P.W. Wanandi, W.M. Davis, C.C. Cummins, J. Am. Chem. Soc. 118 (1996) 10175;
(b) For molybdenum see: A.R. Johnson, P.W. Wanandi, C.C. Cummins, Organometallics 13 (1994) 2907;
(c) E.L. Sceats, J.S. Figueroa, C.C. Cummins, M.M. Loening, P. van der Wel, R.G. Griffen, Polyhedron 23 (2004) 2751;
(d) W. Zhang, S. Kraft, J.S. Moore, Chem. Commun. (2003) 832;
(e) T. Agapie, P.L. Diaconescu, C.C. Cummins, J. Am. Chem. Soc. 124 (2002) 2412;
(f) A. Fuerstner, C. Mathes, C.W. Lehmann, Chem. Eur. J. 7 (2001) 5299;
(g) J.B. Greco, J.C. Peters, T.A. Baker, W.M. Davis, C.C. Cummins, G. Wu, J. Am. Chem. Soc. 123 (2001) 5003;
(h) A. Fuerstner, C. Mathes, C.W. Lehmann, J. Am. Chem. Soc. 121 (1999) 9453.
[12] D.C. Bradley, I.M. Thomas, J. Chem. Soc. (1960) 3857.
[13] T. Tanaka, T. Onoue, K. Kamei, K. Murakami, C. Iwata, J. Chem. Soc., Chem. Commun. (1990) 906.
[14] H. Ohno, K. Hiramatsu, T. Tanaka, Tetrahedron Lett. 45 (2004) 75.
[15] D. Seebach, L. Widler, Helv. Chim. Acta 65 (1982) 1972.
[16] A. Sato, A. Hattori, K. Ishihara, S. Saito, H. Yamamoto, Chem. Lett. 32 (2003) 1006.
[17] S. Saito, H. Yammoto, Chem. Commun. (1997) 1585.
[18] R. Imwinkelreid, D. Seebach, Org. Synth. 67 (1989) 180.
[19] A. Shah, A. Singh, R.C. Mehotra, Polyhedron 5 (1986) 1285.
[20] A. Shah, A. Singh, R.C. Mehotra, Indian J. Chem. A 32 (1993) 632.
[21] H. Noeth, M. Schmidt, Organometallics 14 (1995) 4601.
[22] S.L. Latesky, J. Keddington, A.K. McMullen, I.P. Rothwell, Inorg. Chem. 24 (1985) 995.

[23] A.J. Nielson, P. Schwerdtfeger, J.M. Waters, J. Chem. Soc., Dalton Trans. (2000) 529.
[24] A.J. Nielson, C. Shen, P. Schwerdtfeger, J.M. Waters, Eur. J. Inorg. Chem. (2005) 1343.
[25] Y. Morino, H. Uehara, J. Chem. Phys. 45 (1966) 4543.
[26] Y.E. Chao, P.M. Rodgers, D.E. Wigley, S.J. Alexander, A.L. Reingold, J. Am. Chem. Soc. 113 (1991) 6326.
[27] (a) P.J. Toscano, E.J. Shermerhorn, E. Barren, S. Liu, J. Zubieta, J. Coord. Chem. (1998) 169;
(b) M.H. Chisholm, J.-H. Huang, J.C. Huffman, W.E. Streib, D. Tiedtke, Polyhedron 43 (1997) 2941;
(c) C. Floriani, F. Corazza, W. Lesueur, A. Chiesi-Villa, C. Guastini, Angew. Chem. 101 (1989) 93.
[28] M. Kol, M. Shamis, I. Goldberg, Z. Goldschmidt, S. Alfi, E. Hayut-Salant, Inorg. Chem. Commun. 4 (2001) 177.
[29] (a) Y. Kim, J.G. Verkade, Organometallics 21 (2002) 2395;
(b) W. Wang, M. Fujiki, K. Nomura, Macromol. Rapid Commun. 25 (2004) 504.
[30] V. Ugrinova, G.A. Ellis, S.N. Brown, Chem. Commun. (2004) 468.
[31] L. Michalczyk, S. de Gala, J.W. Bruno, Organometallics 20 (2001) 5547.
[32] (a) M.G. Davidson, C.H. Doherty, A.L. Johnson, M.F. Mahon, Chem. Commun. (2003) 1832;
(b) A.J. Nielson, C. Shen, J.M. Waters, Acta Crystallogr., Sect. C 59 (2003) m494.
[33] A. Lehtonen, R. Sillanpaeae, Organometallics 24 (2005) 2795.
[34] K.C. Fortner, J.B. Bigi, S.N. Brown, Inorg. Chem. 44 (2005) 2803.
[35] R.H. Blessing, Acta Crystallogr., Sect. A 51 (1995) 33.
[36] G.M. Sheldrick, Acta Crystallogr., Sect. A 46 (1990) 467.
[37] G.M. Sheldrick, Program for the Refinement of Crystal Structures, University of Göttingen, Göttingen, Germany, 1997.
[38] L.J. Farrugua, ORTEP-3 for Windows, Version 1.06, University of Glasgow, Scotland, UK.
[39] H.J. Bernstein, C. Duque, G. Grossman, M. Molinaro, A. Mueller, N. Salame, R. Sayle, P. Valadon, RASTOP, version 2.1 – September 14 (P. Valadon, P.O. Box 13014, La Jolla, CA 928064, USA), 2004.